

System Performance Simulations of the RatCAP Awake Rat Brain Scanner

Sepideh Shokouhi, Paul Vaska, David J. Schlyer, Sean P. Stoll, Azael Villanueva, Jr., Aarti Kriplani, Craig L. Woody, *Member, IEEE*, and Nora Volkow

Abstract— We are evaluating the image reconstruction capabilities of RatCAP by using different modified versions of SimSET (Simulation System for Emission Tomography). We have been able to model the proposed tomograph that will consist of lutetium oxyorthosilicate (LSO) crystals arranged in 12 4x8 blocks and have investigated how far the RatCAP's ring diameter (~ 40 mm) and its block detector geometry will affect its image reconstruction for small animal studies. Since the field of view will be almost as large as the ring diameter, radial elongation artifacts due to parallax error are expected to degrade the spatial resolution and thus the image quality at the edge of the FOV. In addition to Monte Carlo simulation, we are presenting some preliminary results of experimentally acquired images in both 2D and 3D modes.

I. INTRODUCTION

Current small animal PET imaging instruments for rats are limited by the need of anesthesia for motion elimination which can profoundly depress brain function [1]. RatCAP will eliminate the motion of the animal relative to the imaging device by reducing the diameter of a tomograph to such an extent that it can be directly attached to the rat's skull. The feasibility of the proposed geometry has been previously analyzed [2]. A detailed description of the RatCAP's design has also been reported in [3].

Although the small diameter of the tomograph (40mm) is advantageous in the sense of reduced cost due to the reduced number of detectors and increased sensitivity due to the increased solid angle coverage, the fact that the field of view

nearly fills the detector ring might lead to severe parallax effects which result in radial elongation artifacts [4].

We acquired data in both 2D and 3D mode. Although operating in 3D would increase the sensitivity, a 2D acquisition can also be considered as a reasonable alternative in terms of maintaining a uniform sensitivity along the axial direction. Furthermore, since the 3D data were Fourier rebinned before applying a 2D filtered back-projection, we would expect to get a better axial resolution in 2D mode than in 3D mode. The data were not pre-corrected for scatter therefore a reasonable energy resolution is necessary for an efficient threshold setting. Even though the small size of a rat's brain causes less in object scattered events, the detected scatter fraction is increased due to the solid angle increase.

This paper will present system performance simulations of this new detector system, along with some preliminary 2D and 3D (Fourier rebinned) [5] images obtained by two detector blocks on a rotational platform that can provide tomographic data.

II. MATERIALS & METHODS

A. Experimental

The final model of RatCAP will consist of 12 LSO-APD detector blocks that are arranged in a ring with a diameter of 40 mm. Each block consists of a 4x8 array of LSO-APD elements. In the current state of our experiment the complete tomographic ring does not exist yet (only 2 out of 12 blocks are available). For preliminary image reconstructions, we have placed a rotational platform between the detectors (Fig. 1). Different phantoms, seen in Fig. 2 have been placed on the center of the platform and rotated in desired angular steps. Unfortunately this approach would allow collecting coincident events only between detector blocks which are directly opposite one another whereas in the real RatCAP, non-opposing detectors are also involved in coincident event detection. This sets a limit on the dimension of the FOV in the current experiment of ~8 mm. One main advantage of using the phantom rotational platform is the ability of representing a complete ring tomograph without any gaps between the detector blocks by decreasing the rotational steps which ensures a complete radial and angular sampling. This is useful because, first of all, sinograms with no zero efficiency bins are more compatible with standard filtered back projection reconstruction methods. Secondly, these complete sinograms can be compared with incomplete real RatCAP sinograms to

Manuscript received May 9, 2003. This work was supported in part by a grant from the DOE Office of Biological and Environmental Research and DOE Contract DE-AC02-98CH10886U.S.

S. Shokouhi is with SUNY @ Stony Brook, Stony Brook, NY USA (telephone: 631-344-4576, e-mail: sepideh@bnl.gov).

P. Vaska is with Brookhaven National Laboratory, Upton, New York 11973 (telephone: 631-344-6228, e-mail: vaska@bnl.gov).

D. J. Schlyer is with Brookhaven National Laboratory, Upton, New York 11973 (telephone: 631-344-4587, e-mail: schlyer@bnl.gov).

S. P. Stoll is with Brookhaven National Laboratory, Upton, New York 11973 (telephone: 631-344-5331, e-mail: stoll@bnl.gov).

A. Villanueva is with SUNY @ Stony Brook, Stony Brook, NY USA (telephone: 631-344-4576, e-mail: azvilla@bnl.gov).

A. Kriplani is with SUNY @ Stony Brook, Stony Brook, NY USA (telephone: 631-344-4576, e-mail: aarti@bnl.gov).

C. L. Woody is with Brookhaven National Laboratory, Upton, New York 11973 (telephone: 631-344-2752, e-mail: woody@bnl.gov).

N. Volkow is with the National Institutes of Health, Bethesda, MD USA, on leave from Brookhaven National Laboratory, Upton, New York 11973 (e-mail: volkow@bnl.gov).

estimate experimentally the impact of detector gaps on the image quality.

For the experimental part, two phantoms (2 point sources & an L-shaped source) were placed on a rotational platform between two detector blocks each comprising a 4 x 8 array of 2 x 2 x 10 mm lutetium oxyorthosilicate (LSO) crystals coupled (via a UV-transparent silicone wafer) to a geometrically matched 4 x 8 APD array from Hamamatsu (model S8550, with 1.6 mm x 1.6 mm active area per element). The sources were 1 mm in diameter stainless steel filled with resin impregnated with Ge-68. The amounts of activity in the two rods are slightly different.

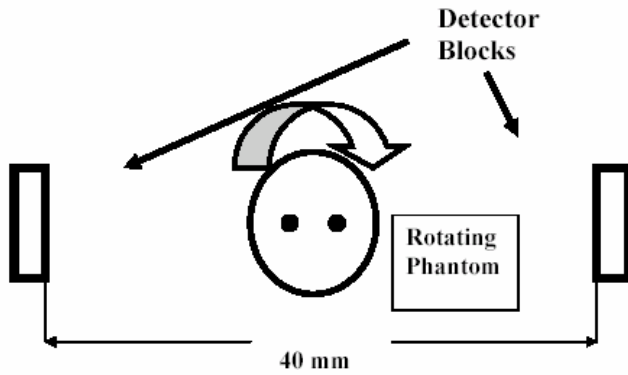


Fig. 1. Phantoms were placed on a rotational platform and rotated in $\sim 3^\circ$ steps from 0 to 180 degree.

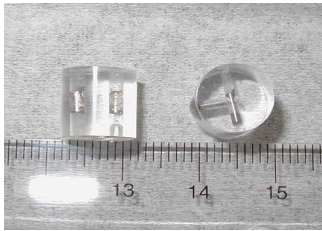


Fig. 2. ^{68}Ge phantoms of two point sources and L-shaped source.

For detecting each coincident event, the APD-output signals from all 64 channels (32 from each detector block) were readout and digitized by CAMAC FERA ADCs (LeCroy 4300B). The pulse height spectra from all channels were plotted and fitted to determine the 511 keV photopeak positions. The value of the peak positions together with channel specific pedestal values were used to make a gain match among the channels. The gain corrected pulse height spectra were used to set an energy threshold at 420 keV. The gain corrected channels with the highest charge output (one channel from each side) was used for event positioning.

The coincident events were binned into 13(angular) x 7(radial) sinograms. For the given field of view, the size of each radial bin (1.2 mm) was almost equal to the half of the detector element pitch size (2.4 mm). A 3D data acquisition and Fourier rebinned (FORE) [5] filtered back projection was

applied and compared with the images of 2D data. Both 2D and 3D images were reconstructed using image reconstruction and analysis software supplied with our Concorde MicroPET system. For each sinogram a header file was created which specified the sinogram parameters. For the 3D data, different reconstruction protocols were created which incorporated maximum ring differences from 0 to 5. The bigger the ring difference, the larger is the co-polar coincidence acceptance angle. The highest possible ring difference is 7 where coincident events between LSO crystals from the furthest axial positions were taken whereas in the case of ring difference =0 the 3D mode reassembles the 2D mode again because only direct sinograms have been taken into account. Since the reconstruction software was written for a R4 MicroPET scanner. The 3D sinograms of RatCAP had to be modified to ensure a correct interpretation of the 3D sinograms by the reconstruction software. One of the parameters that caused misinterpretations was the span value that gives the compression factor of the oblique sinograms in co-polar direction. For MicroPET that has larger number of axial detector elements (32) relative to RatCAP (8), spans bigger than one are reasonable whereas in RatCAP span=1 (no compression) is required.

Unfortunately, span =1 is not accommodated by the image reconstruction software leading to a mis-positioning of the point sources in the axial direction. We have zero-padded the sinograms in order to address this problem. Table I gives a summary of some adjusted parameters in the header file and reconstruction protocol for both 2D and 3D. The experimental conditions require no arc corrections.

TABLE I
DATA ACQUISITION PARAMETERS

Data mode	2D	3D	3D	3D
image planes	8	15	15	15
Max.ring difference	0	1	3	5
Span	1	1	1	1

B. Simulations

By using Monte Carlo techniques for PET tomographic applications, positron sources of different sizes and shapes can be generated and their annihilation photons tracked within the tomograph. We have used SimSET (Simulation System for Emission Tomography) for the RatCAP simulations. The SimSET package has been developed by the Imaging Research Laboratory at the University of Washington [6]. It is written in a modular format. For PET simulations, 3 modules were required. The first module is the Photon History Generator (PHG) where the generation and transportation of photons within the user-defined object are tracked. This module is followed by the detector module where the detector geometry and material is specified. The last module is the binning module that takes care of the detection records and creates output files. We used SimSET versions 2.6.2.2 -2.6.2.4. Since none of these versions provides block detector geometry, we modified some of its codes to closely simulate a block detector

geometry based on using a cylindrical PET in the detector module and writing a routine to simulate the behavior of a discrete-crystal block-detector tomograph. The original (not modified) cylindrical PET option models a tomograph with a depth of interaction measurement capability because the coincident events are binned based on their exact interaction position within a LSO-crystal cylinder.

The discretization process can be described as a nearest crystal selection for each of the two gamma-rays in coincidence, based on the input block structure. A valid event is binned into 3D sinograms according to segment in the standard way. The user can define how (and whether) to do discrete crystal-binning in a parameter file. Two different discretization methods have been developed. The earlier code did not take the gaps between the detector blocks in account. This version was used to estimate the impact of the LSO crystal length on the parallax error, where only the relation between the uncertainty in depth of interaction DOI (given in crystal length) and the radial elongation in a small tomograph was the main interest. Two different crystal lengths (5mm and 10 mm) were modeled and compared with each other (Fig. 7). A cylindrical PET with a diameter of 40 mm and a thickness of 5(10) mm had been segmented in 58 discrete elements. The choice of 58 segments was to accommodate the pitch size of a realistic LSO detector element. Several point sources with different positions within the FOV have been generated. The positions of the point sources were shifted from the center of the tomograph towards the edge of the FOV. The interaction position of the annihilation photons within each crystal segment was assigned to its center point at the depth of 1/2 the crystal thickness. The resultant coincident events were binned in 29 (angular) x 33 (radial) sinograms which have been normalized and reconstructed. The normalization was done by using a thin line source (Fig. 3a) taking the projection perpendicular to the line source and using the intensity profile (Fig. 3b) to correct the response along the line.

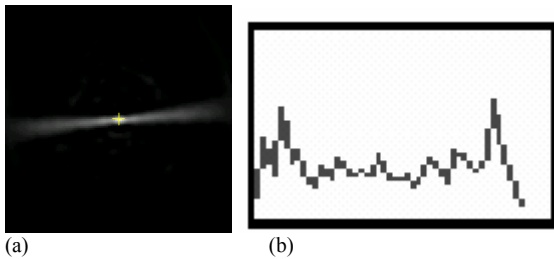


Fig. 3. A line source (a) was generated and its intensity profile (b) at the projection perpendicular to the line source was used for normalization. The slight angular shift in (a) is due to the discretization and the assignment of counts to the center of each segment.

After reconstruction, the FWHM of each point source in the radial direction has been measured and plotted as a function of its distance from the center of the tomograph.

The second version of the discretization had been developed later and took the realistic gaps between the detector blocks in account. This version is a closer approximation to the RatCAP

design and it will be used to model the probability matrix of RatCAP for ML-EM [7] image reconstruction. This discretization code places a grid of rectangular crystals organized in evenly spaced blocks over the original SimSET's cylindrical detector, rejecting events which don't fall within the blocks.

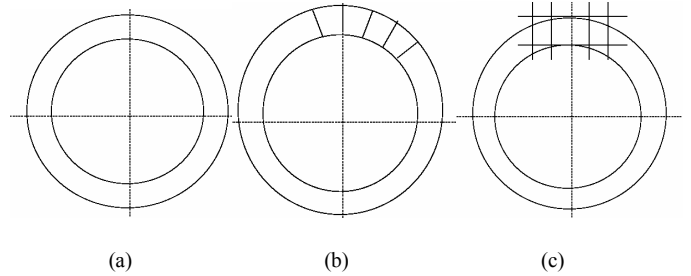


Fig. 4. (a) Cylindrical PET, (b) discretized PET with no gaps, (c) discretized PET with gaps between blocks (block detector geometry).

RatCAP's geometry leads to incomplete sampling of the experimental data that result into zero efficiency bins (ZEBs). None of the modified SimSET versions could be used to efficiently model the characteristic RatCAP patterns. The first discretization method (Fig. 4b) ignores the gaps at all and the second method although models the gaps, re-bins the events in a way that the sinograms have no zero efficiency bins but need to be Arc corrected before reconstructing with Filtered back projection. Here we just used the unmodified Cylindrical PET to create several activity objects with diameters between 1 and 4 mm, placed in different positions inside a field of view of about 36 mm. The resulting sinogram was multiplied by a pattern sinogram to create a realistic RatCAP sinogram with expected unnormalizable zero efficiency bins (Fig. 8b). We performed a nearest neighbor 1D interpolation to compensate the effect of the gaps. The interpolated image (Fig. 8c) was then compared to the idealistic cylindrical PET with no gaps (Fig. 8a). The simulated acquisition was taken in 2D mode and the images were reconstructed by using a 2D filtered back projection.

III. RESULTS

First images of the phantoms (Fig. 3) on the rotational platform:

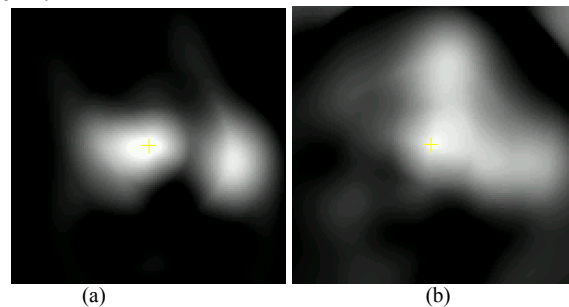


Fig.5. Image of two-point source (a) and L-shaped source (b),. Normalization of the image is under development.

Both 2D and 3D (Fourier rebinned) were compared

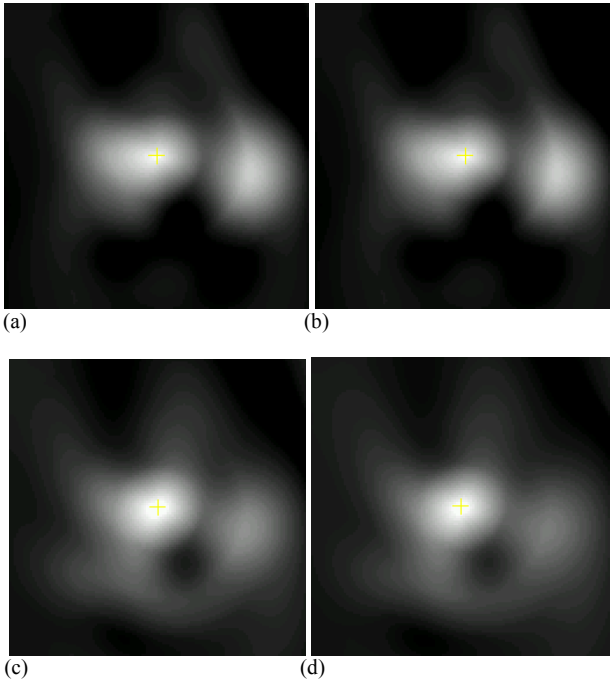


Fig. 6. Image of two-point sources: (a)... 2D data mode, (b)... 3D mode with ring difference =1, (c)... 3D mode with ring difference =3, (d)... 3D mode with ring difference =5. The image normalization is under development

The sinograms of the two phantoms were obtained by rotating the phantoms on the rotational platform in 13 steps. Images were reconstructed by applying filtered back projection and the measured point spread function was approximately 2.1 mm FWHM. The point sources are 5 mm apart from each other and can be easily resolved in the image (Fig. 6). Similar measurements with a single point source have been made and reported [3].

Effect of the crystal length on the radial elongation:

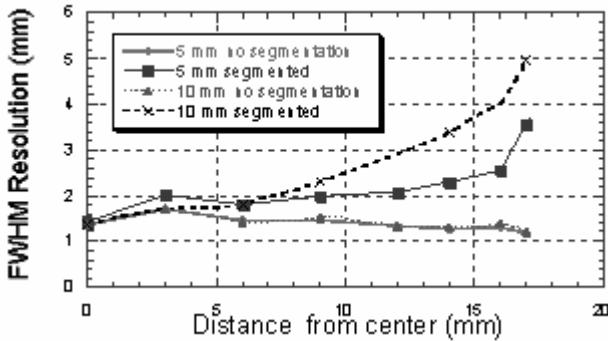


Fig. 7. Point-spread function of a point source as a function of its distance from the center of the FOV for 4 different detector configurations: 1) RatCAP (40 mm ID) and 5 mm LSO crystal length, 2) RatCAP (40 mm ID) and 10 mm LSO crystal length, 3) Tomogarth with depth measurement capability (40 mm ID) and 5 mm LSO crystal length, and 4) Tomogarth with depth measurement capability (40 mm ID) and 10 mm LSO crystal length.

The effects of incomplete sampling in the RatCAP simulation

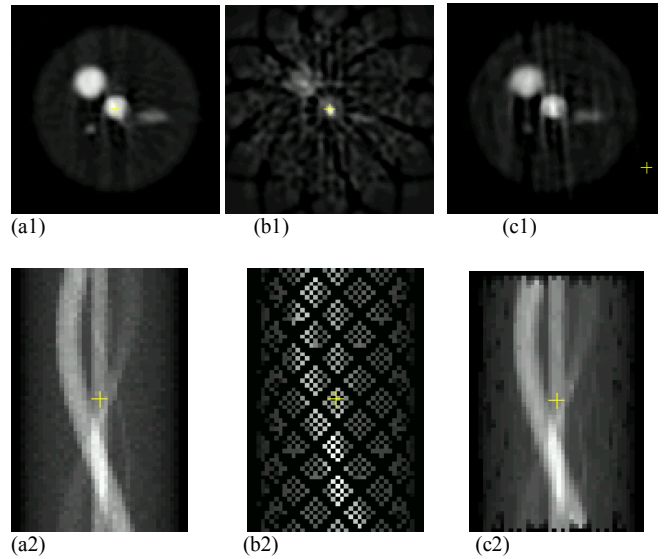


Fig. 8. (a1) Reconstructed image from a fully sampled sinogram(a2). (b1) Reconstructed image from a realistic RatCAP geometry sinogram(b2). (c1) Reconstructed image from interpolated sinogram(c2).

IV. CONCLUSION

The first images of an incomplete RatCAP tomograph by using a rotational platform and 2 LSO-APD detector blocks have been acquired. These first preliminary results prove the ability of RatCAP to provide acceptable image quality both in 2D and 3D mode. There were no septa incorporated in 2D mode. The lack of using septa is compensated by setting an energy threshold at 420 keV to cut off scattered events and the superior event positioning at high count rates due to the one-one correspondence between the crystals and the APD pixels. This seems to be compatible with Fourier rebinned 3D data as long as the ring difference of the oblique LORs does not exceed 5 rings that correspond to an axial aperture of about 20 degrees. This may be because the 3D sinogram data should be pre-corrected for attenuation, scatter, random and normalization before doing a Fourier rebinned filtered back projection.

Our group is currently working by improvement of the energy resolution of the LSO-APD [8] and reconstruction techniques such as ML-EM [7]. Many expected effects such as the presence of artifacts were evaluated by using a modified SimSET that is capable of representing a block detector tomograph. We came to the conclusion that by incorporating 5mm crystals we can maintain a relative constant radial resolution up to 12 mm away from the center of the tomograph (Fig. 7).

This radius is large enough to cover the entire region of the rat's brain [3]. The reduction of the crystal length is a simple alternative to the placement of additional photo sensors to determine the depth of interaction information. The latter approach would not be easily technically compatible with the RatCAP dimensions. Our simulation results show that the resolution can be improved from 2.3 mm to 1.8mm at a distance from the center of 9 mm by using a 5mm long crystal

instead of a 10 mm crystal. This improvement in resolution comes at cost of an approximate factor of 4 in coincidence sensitivity, unless a second layer of crystals is used. The selection of 5mm crystals has another effect on the tomograph performance in terms of its energy resolution. This result has been reported in [8], where the measured energy resolution of 5 mm detector arrays were significantly improved comparing with 10 mm crystals.

Another characteristic of RatCAP is the presence of the unnormalizable zero efficiency bins which has been modeled by using SimSET. Interpolation methods should be applied when analytical methods of image reconstruction are used.

V. ACKNOWLEDGEMENTS

The authors sincerely acknowledge Proteus and CTI, Inc. This work is a collaboration between Brookhaven National Lab, and Stony Brook University and is supported under a grant from the DOE Office of Biological and Environmental Research and DOE Contract DE-AC02-98CH10886

VI. REFERENCES

- [1] K. S. Hendrich, P. M. Kochanek, J. A. Melick, J. K. Schiding, K. D. Statler, D. S. Williams, D. W. Marion, and C. Ho, "Cerebral perfusion during anesthesia with fentanyl, isoflurane or pentobarbital in normal rats studies with arterial spin-labeled MRI," *Magnetic Resonance in Medicine*, vol. 46, pp. 202-206, 2001.
- [2] P. Vaska, D. J. Schlyer, C. L. Woody, S. P. Stoll, V. Radeka, and N. Volkow, "Imaging the unanesthetized rat brain with PET: A feasibility study," *2001 IEEE Nuclear Science Symposium and Medical Imaging Conference*, vol. 3, pp. 1569-1571, 2001.
- [3] P. Vaska, C. L. Woody, D. J. Schlyer, S. Shokouhi, S. P. Stoll, J. F. Pratte, P. O'Connor, S. Rescia, B. Yu, A. Villanueva Jr., A. Kriplani, A. Prakash, V. Radeka, and N. Volkow, "RatCAP: Miniaturized head-mounted PET for conscious rodent brain imaging," Poster M3-7 *IEEE Medical Imaging Conference*, Oct. 19-26, 2003.
- [4] W.W. Moses, P.R.G. Virador, S.E. Derenzo, R.H. Huesman, and T.F. Budinger, "Design of a high-resolution, high-sensitivity PET camera for human brains and small animals," *IEEE Trans. Nuclear Science*, Vol. 44, No. 4, August 1997.
- [5] M. Defrise, M. Sibimana, P. E. Kinahan, D. W. Townsend, C. Michel, M. Sibomana, and D.F. Newport, "Exact and approximate rebinning algorithms for 3-D PET data," *IEEE Trans. Med. Imaging*, Vol. 16 No. 2, pp. 145-58.
- [6] T. K. Lewellen, R. L. Harrison, and S. Vannoy, "The SimSET program," in *Monte Carlo Calculations in Nuclear Medicine, Medical Science Series*, M. Liungberg, S. E. Strand, and M. A. King, Eds. Bristol: Institute of Physics Publishing, 1998, pp. 77-92.
- [7] L.A. Shepp, and Y. Vardi, "Maximum likelihood reconstruction in emission tomography," *IEEE Trans. Med. Imaging*, MI-1 (1982), pp. 113-122.
- [8] A. Kriplani, S. P. Stoll, S. Shokouhi, D. J. Schlyer, A. Villanueva Jr., P. Vaska, and C. L. Woody, "Comparison of experimentally measured light output with Monte Carlo simulations from LSO crystals" Poster M14-183, *IEEE Medical Imaging Conference*, Oct. 19-26, 2003.